Understanding Ti intermediate-band formation in partially inverse thiospinel $MgIn_2S_4$ through many-body approaches

I. Aguilera,[1,2] Pablo Palacios,[1,3] and P. Wahnón[1,2]

[1]*Instituto Energía Solar, ETSI Telecomunicación, UPM, Ciudad Universitaria, Madrid E-28040, Spain*

[2]*Dpt. Tecnologías Especiales, ETSI Telecomunicación, UPM, Ciudad Universitaria, Madrid E-28040, Spain*

[3]*Dpt. Física y Química Aplicadas a la Técnica Aeronáutica, E. de Ingeniería Aeronáutica y del Espacio, UPM, Ciudad Universitaria, Madrid E-28040, Spain*

(Received 25 May 2011; revised manuscript received 27 July 2011; published 12 September 2011)

Indium atoms in octahedral sites are substituted by Ti atoms in spinel $MgIn_2S_4$, where d states of Ti form an intermediate band. However, the complex spinel structure of the host semiconductor requires a supercell study of the intermediate-band compound. Self-consistent many-body approaches are applied to the smaller cell of this material, starting from the static Coulomb-hole and screened-exchange approximation to the GW approach and then carrying out a perturbative GW calculation. We discuss the influence of many-body effects on the formation of the intermediate band through a comparison with density functional theory (DFT) and DFT + U. We find that both the self-consistent parameter-free many-body and DFT + U + G_0W_0 calculations indicate that only a totally occupied intermediate band can be formed by Ti in inverse $MgIn_2S_4$. This justifies the use of DFT + U + G_0W_0 to treat the supercells, when the self-consistent GW is not affordable.

DOI: 10.1103/PhysRevB.84.115106 PACS number(s): 71.55.Ak, 71.10.−w, 71.15.Mb, 71.20.Be

I. INTRODUCTION

In the last few years, several intermediate-band materials have been proposed as potential candidates for high-efficiency solar cells. Thin-film technology combined with the intermediate-band (IB) concept represents one of the most promising concepts in the quest for more efficient, lower-cost solar cells.

The intermediate-band concept was proposed as a solution to the efficiency problem because a partially filled narrow band that is isolated from the valence and conduction bands of a host semiconductor would allow the absorption of sub–band-gap energy photons. For a solar cell, this would result in the creation of additional electron-hole pairs and, in principle, in an increase in photocurrent without a decrease in open-circuit voltage. A cell based on such an approach could reach theoretical efficiencies up to 63.2%.[1]

However, a greater absorption of photons does not necessarily mean a greater photocurrent, as very localized levels could favor nonradiative recombination. Therefore, in order to be efficient, an intermediate band has to fulfill some requirements. It has to have a small dispersion and must not be a discrete level; however, at the same time, it has to be narrow enough to be well isolated from the valence and conduction bands to avoid thermalization to the IB. It also has to be partially filled to allow comparable rates for the two possible absorption processes involving the IB. In addition, the material studied here has advantage of spin polarization, as the spin selection rules for electronic transitions can improve the enhancement in lifetimes for the generated electron-hole pairs.[2]

Note that the use of two low-energy photons to achieve the excitation of one electron across a higher-energy gap already operates in natural photosynthesis; the IB concept behaves differently, however, in that both photons are absorbed by the same system, and the direct high-energy excitation of an electron through absorption of a shorter-wavelength photon is still possible. Note also that this concept could also improve the efficiency of photocatalytic processes, which is based on the transfer of photogenerated electrons and holes to molecules adsorbed on surfaces, as a wider range of the light spectrum could be used thanks to the IB.

Some of the first proposals to carry out the IB concept were based on quantum dots (see, e.g., Ref. 3 and references therein) and, although proof of concept of the principle could be obtained with them,[4] the perspectives of achieving an efficient system on this basis seem slight as the absorbing centers are very diluted, leading to rather small absorption coefficients. Thus, single-phase materials allowing higher concentrations of IB-forming components are preferable. According to this, several doped semiconductors have been proposed to form the appropriate IB materials. O-doped (Zn,Mn)Te and N-doped Ga(As,P) have been claimed, on the basis of spectroscopic data interpreted with a band anticrossing model, to form IB structures,[5,6] although full first-principles quantum calculations were not made on these systems.

On the other hand, previous works by the present authors have shown that IB materials can be obtained if judiciously chosen transition metals are inserted into certain semiconductors.[7,8] In silicon this can be achieved with interstitial Ti atoms, and the calculation results[9] agree with experimental data obtained on specimens made by ion implantation of Ti in high doses in Si wafers.[10] The substitutional insertion of significant amounts of S or Se in Si, as achieved recently in the laboratory,[11] can also produce adequate IB materials when coupled with p-doping.[12] However, Si is not the best host material for implementing the IB concept, since its band gap is much smaller than the optimum one that would allow the maximum efficiency to be obtained in an IB photovoltaic cell, and therefore these Si-based systems are useful mainly in fundamental studies of the IB principle. Only by resorting to metastable Si polymorphs, such as the type-II Si clathrates that have $E_g = 1.9$ eV,[13] can silicon lead to an optimum IB material.

The first materials proposed to combine the intermediate-band concept with thin-film technologies (intended to

reduce the costs) were derivatives of chalcopyrites. Studies of intermediate-band materials based on $CuGaS_2$ have already been presented,[14] showing a potential suitability for enhanced photovoltaic applications. In these materials, Ga atoms were replaced by Ti or Cr (at tetrahedral sites). It is well known[15] that the octahedral environment is thermodynamically more stable for these transition metals. This is because there is a preference to be surrounded by six atoms rather than by four.

Recently, we presented results of the spinel semiconductor In_2S_3, where octahedral In atoms were replaced by V or Ti.[15] V-substituted In_2S_3 was synthesized later, due to our promising predictions. This allowed a partially filled intermediate-band material, absorbing across the full solar spectrum range, to be synthesized.[16]

The compound we are studying here is derived from a semiconductor usually grown as thin films as well: the thiospinel $MgIn_2S_4$, which has an experimental band gap of 2.1–2.28 eV,[17,18] close to the optimum gap for thin-film IB solar cells.[19] In this compound, some of In atoms are substituted in octahedral sites by Ti. Previous generalized gradient approximation (GGA) calculations indicated the possibility of Ti d states forming an intermediate band in this semiconductor.[15,20] In order for this IB to be efficient, it has to be isolated energetically from the valence band (VB) and the conduction band (CB) of the host semiconductor. However, Ti substitution in $MgIn_2S_4$ has only been studied at the GGA level, and a Ti intermediate band is predicted in GGA to overlap with the CB.

Because of the scarcity of experimental results of IB materials and since high precision in electronic structures is not achieved using standard density functional theory (DFT), many-body approaches are necessary to determine whether an isolated intermediate band can be formed in this compound.

We present self-consistent Coulomb-hole and screened-exchange (COHSEX)[21] calculations followed by a perturbative GW (G_0W_0) for this intermediate-band material. The COHSEX + G_0W_0 scheme has been successfully tested for metals, semiconductors, insulators, and even prototypes of strongly correlated systems.[22–26] It leads to quasiparticle band gaps and band structures in very good agreement with the experiments and with full self-consistent GW calculations made using the scheme established by Faleev *et al.*[27] In all cases, self-consistent many-body calculations are very expensive and not affordable for most IB materials. In order to see whether the results of self-consistent GW calculations can be reproduced with a DFT-based approach (at a significantly reduced expense), we have also carried out GGA + U calculations.

The spinel structure of $MgIn_2S_4$ has a so-called normality index, defined as the number of Mg atoms in tetrahedral sites per chemical formula: 0 for the so-called inverse structure, 1 for the direct (or normal) one, and in-between values for partial situations.[28] $MgIn_2S_4$ is assumed to have an experimental normality index of $x = 0.16$ in nature.[29,30] For the representation of a value of the normality close to that of the experiments, a 42-atom supercell is used. Self-consistent many-body approaches are prohibitive for this supercell and therefore, in this work, we will also use the fully inverse structure, with 14 atoms in the unit cell for computational reasons. In both cells, one In atom at an octahedral site is substituted by Ti, giving stoichiometry $Mg_6TiIn_{11}S_{24}$($x = 0.167$) and $Mg_2TiIn_3S_8$ ($x = 0$).

II. COMPUTATIONAL DETAILS

Local density approximation (LDA) to DFT and many-body calculations were carried out with the ABINIT code[22,31] using norm-conserving pseudopotentials[32] generated through the *fhi98PP* code.[33] Semicore states (i.e., $4s4p4d$ for In and $3s3p$ for Ti) were taken into account explicitly in the valence. It has been shown[34] that this may substantially affect results for GW calculations.

LDA results were used as the starting point for a self-consistent COHSEX calculation and the latter for a dynamic G_0W_0 step. For COHSEX and G_0W_0, a basis set of around 30 000 plane waves was required for convergence and a Monkhorst-Pack **k**-point mesh of $3 \times 3 \times 3$ was used to sample the Brillouin zone (BZ). This corresponds to 14 **k** points in the irreducible BZ. For the G_0W_0 calculations the plasmon-pole model[35] was adopted. The self-consistency in the COHSEX calculations was stopped when differences between eigenvalues in one cycle and the previous one were lower than 0.015 eV.

As GW corrections were obtained only for 14 **k** points and, after checking corrections, were slightly **k**-point dependent, they were interpolated using a quadratic interpolation for the denser **k**-point mesh needed for the representation of densities of states.

GGA + U and GGA + U + G_0W_0 calculations were carried out using with the VASP plane-wave code[36] and using the Perdew-Wang 1991 functional[37] for GGA and projector-augmented waves (PAW) pseudopotentials.[38] In order to see how the use of different pseudopotentials for VASP and ABINIT may affect results, we performed an LDA calculation within the same conditions with both codes. We found that the differences are very small and can be neglected for the purposes of this work (see supplementary material).[39]

Results for the direct spinel structure of this compound obtained with GGA + U, where U was calculated self-consistently with the method detailed in Refs. 40, 41, were presented in Ref. 42. We have used a value of U that reproduces with VASP the density of states (DOS) obtained in Ref. 42. This value has been found to be $U = 1.8$. All GGA + U and GGA + U + G_0W_0 calculations in this work have been carried out with that value of U and under the assumption that U will not vary significantly from the direct to the inverse structure.

Full relaxations of cells and ion positions were carried out in all cases. LDA, LDA + G_0W_0, COHSEX, and COHSEX + G_0W_0 are carried out in the LDA-relaxed structure ($a = 10.52$ Å), whereas GGA, GGA + U, and GGA + U + G_0W_0 were carried out in the GGA structure ($a = 10.76$ Å). We have previously checked that the differences between these two structures do not significantly affect the density of states for this material (see supplementary material).[39]

III. RESULTS AND DISCUSSION

A. Full inverse structure for comparison of approaches

In order to study how the intermediate band is formed beyond DFT and which characteristics it has, we have carried out and compared calculations with different approaches. Figure 1 shows densities of states of $Mg_2TiIn_3S_8$ obtained with LDA, GGA, LDA + G_0W_0, COHSEX, COHSEX + G_0W_0, GGA + U, and GGA + U + G_0W_0.

In LDA and GGA [Figs. 1(a) and 1(b)], spin-up electronic structures present, at the Fermi energy, a narrow band formed by the t_{2g} manifold of Ti, whereas the e_g states are highly hybridized with the conduction band. For spin-down, all d states of the transition metal are empty and hybridized with the conduction band of the host semiconductor. These densities of states are in agreement with previous GGA works.[20]

Ti atoms in $MgIn_2S_4$ are surrounded by a octahedron made up of six S atoms. When the Ti is substituted in the direct spinel structure of $MgIn_2S_4$, all six S atoms are equivalent (each of them tetrahedrally coordinated to one Ti, one Mg, and two In atoms) and the octahedron is regular. However, in our case, Ti is substituted in the inverse spinel structure (which is closest to the experiment) in which all six S atoms surrounding the Ti are not equivalent (4 of them are coordinated as in the direct structure, but the other two have one Ti, one In, and two Mg as first neighbors instead). This results in a distortion of the octahedron in one direction that translates into a splitting of the t_{2g} manifold into two branches: a lowest t_{2g} state (fully occupied) that will constitute the IB, and two empty t_{2g} states with higher energy interacting with the CB. Other structural distortions have a slight effect on the splitting of the t_{2g} manifold. The structure of the inverse spinel after the substitution with the transition metal can be seen in Fig. 2.

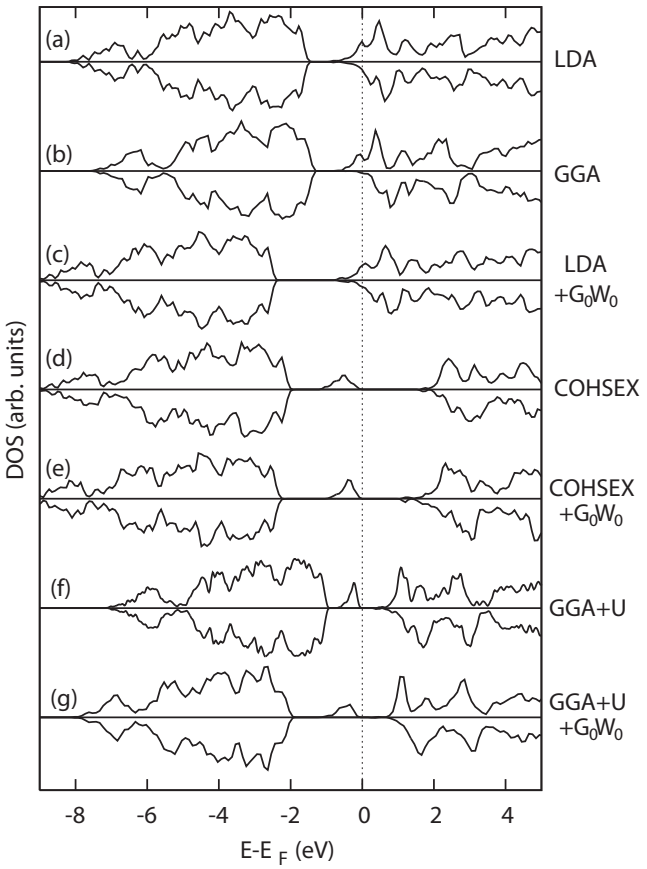

FIG. 1. Comparison of (a) LDA, (b) GGA, (c) LDA + G_0W_0, (d) COHSEX, (e) COHSEX + G_0W_0, (f) GGA + U, and (g) GGA + U + G_0W_0 densities of states of $Mg_2TiIn_3S_8$ aligned at the Fermi energy, which is shown as a dotted black line.

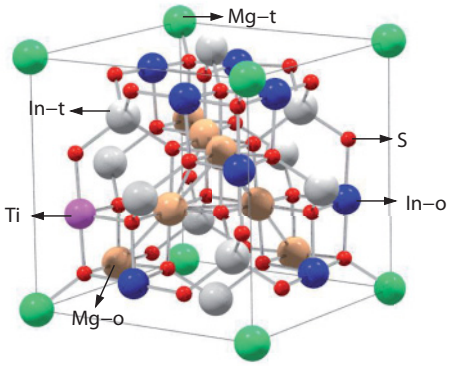

FIG. 2. (Color online) Structure of inverse Ti-substituted $MgIn_2S_4$. In the labels of the species, –t and –o mean tetrahedral and octahedral sites, respectively.

The t_{2g} splitting is already perceptible at the LDA or GGA[20] level, since there is a direct band gap between the two branches of the t_{2g} manifold for any **k** point. However, the indirect band gap is negative within these two approaches. Table I shows the value of the splitting, E_{IC}, between the spin-up occupied t_{2g} band (IB) and the two empty t_{2g} bands (CB), together with the band gap from VB to IB, E_{VI}, and the width of the IB for all the approaches used. The meaning of these band gaps and their direct or indirect character is clarified in the band diagrams in Fig. 3.

Both the LDA and GGA predict a metallic compound in which there is no isolated intermediate band since the d states of the Ti interact with the CB of the host. Since this overlap comes from the underestimation of band gaps in standard DFT, we carried out a perturbative GW calculation using LDA wave

TABLE I. Second column gives the direct energy gaps (E_{VI}) between the top of the VB states of the host semiconductor and the Ti spin-up occupied t_{2g} band (IB). Third column gives the gap (E_{IC}) between the IB and the two empty t_{2g} bands (CB). These latter gaps are indirect (bottom of the CB at the Γ point to top of the IB at W). Width of the IB is Δ_I. All values are in eV.

	E_{VI}	E_{IC}	Δ_I
LDA	0.84	negative	0.87
GGA	0.70	negative	0.89
LDA + G_0W_0	1.68	negative	1.03
COHSEX	1.22	1.88	0.55
COHSEX + G_0W_0	1.44	1.18	0.71
GGA + U	0.34	0.31	0.60
GGA + U + G_0W_0	1.18	0.75	0.61

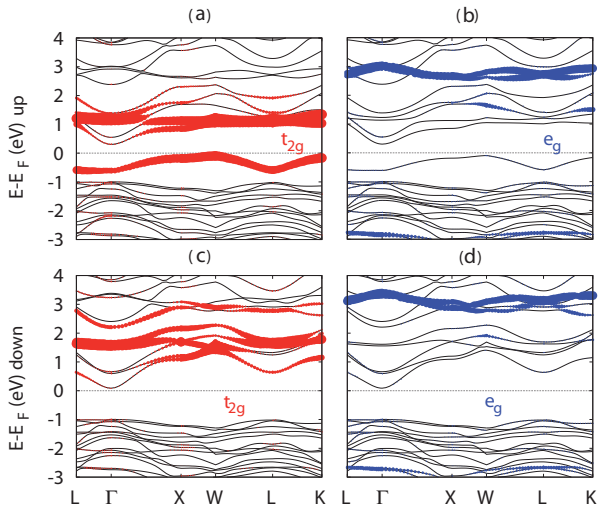

FIG. 3. (Color online) GGA + U band diagram of $Mg_2TiIn_3S_8$. The size of the circles is proportional to the Ti e_g or t_{2g} character of the band. (a) Spin-up states, t_{2g} character; (b) spin up, e_g; (c) spin down, t_{2g}; (d) spin down, e_g.

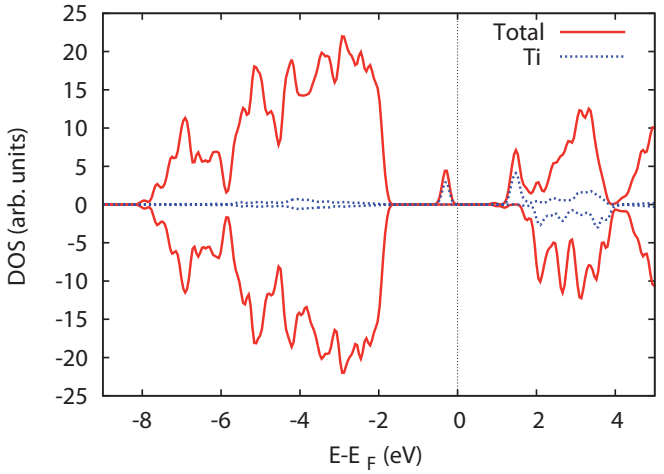

FIG. 4. (Color online) Total (solid) and Ti-projected (dashed) density of states of $Mg_6TiIn_{11}S_{24}$ with normality index 0.16, calculated within the GGA + U + G_0W_0 approach.

functions and eigenvalues to construct G and W. The LDA is, in general, an incorrect starting point for compounds with d electrons.[22,43] It can be seen in Fig. 1(c) that G_0W_0 is not able to open a band gap between the occupied t_{2g} band and the empty ones because, when the screening is obtained using LDA wave functions and energies, the screening thus obtained can be highly overestimated as a result of the underestimation of the LDA band gap, leading to very small G_0W_0 corrections and, therefore, to very small band gaps. The interaction of the IB with the CB in LDA makes the LDA wave functions substantially wrong as a starting point for G_0W_0 and only a self-consistent update of the wave functions will give accurate many-body results.

For this reason we have carried out a self-consistent COHSEX calculation, since COHSEX wave functions have been shown[22] to be much closer to the full self-consistent GW[27] wave functions than those of the LDA. COHSEX has been thus used as a starting point for G_0W_0. We can see in the COHSEX and COHSEX + G_0W_0 densities of states [Figs. 1(d) and 1(e)] that, for spin down, the empty d states of the transition metal hybridize with the bottom of the CB of the host semiconductor (which is mainly of an S p and In s character).

The different theories have little effect on the spin-down states, only differences in the band gap and small differences in the hybridization of the empty d states with the bottom of the CB can be observed. For both spins, the features and widths of the valence-band DOS (mainly made up of states of the host semiconductor) are almost unchanged both in COHSEX and COHSEX + G_0W_0 with respect to the LDA. The main change concerns the spin-up intermediate band, which is now completely isolated from the VB and the CB in contrast to LDA. The inclusion of many-body effects results mainly in an opening of the band gap between the spin-up occupied t_{2g} band and the two empty t_{2g} bands (see Table I), giving a totally occupied isolated intermediate band. The width of this IB is predicted by COHSEX + G_0W_0 to be 0.71 eV.

The total band gap (from the last VB of the host semiconductor to the CB) is 3.3 eV, as compared to the band gap found with COHSEX + G_0W_0 for the host semiconductor, which is 3.1 eV. The experimental band gap of this semiconductor ranges from 2.1 to 2.28 eV,[17,18] which is much smaller than that predicted by GW. It has to be taken into account that experimental results are for optical band gaps, whereas GW is meant for the calculation of quasiparticle band gaps. Therefore, there are two fundamental factors (beyond the precision of the method itself) which may contribute to this difference between GW (quasiparticle) and experimental (optical) band gaps. The main difference is expected to be the result of neglecting the excitonic and polaronic effects. Although there is no clear experimental evidence of excitonic or polaronic effects, the absorption spectra of Ruiz-Fuertes *et al.*[44] seem to be coherent with the presence of excitons, and the large difference $\epsilon_0 - \epsilon_\infty$ ($\epsilon_0 = 18.8$ to 20.74 and $\epsilon_\infty = 5.5$ to 5.8)[18,29] is an indication of significant polaronic effects.[26,45] To a lesser extent, the differences between the LDA and the experimental structural parameters, the finite temperature of the experiments, and the presence of defects (mainly Mg vacancies),[29] may contribute to the difference between the band gaps.

These self-consistent many-body calculations are prohibitive for IB materials with larger cells. We have studied the substitution of one Ti atom in a 14-atom cell but this concentration of Ti is much larger than concentrations expected to be found experimentally. The study of intermediate-band materials with realistic concentrations of transition metals demands the use of DFT-based approaches. Additionally, the normality index that $MgIn_2S_4$ presents in nature can only be reached with a cell of at least 42 atoms. In order to see whether results of self-consistent GW can be reproduced with a DFT-based approach, we have carried out GGA + U calculations.

GGA + U results [with $U = 1.8$, see Fig. 1(f)] show a totally occupied isolated IB in agreement with COHSEX + G_0W_0. Figure 3 details the band diagram obtained with

GGA + U for $Mg_2TiIn_3S_8$ together with the projection of the bands, where the size of the circles is proportional to the t_{2g} (left panels) or e_g (right panels) character of the band. We can also see the indirect character of the band gap since the bottom of the CB is located at the Γ point, whereas the top of the IB is found at the W symmetry point.

However, when comparing it with COHSEX + G_0W_0, the GGA + U band gaps are largely underestimated. In order to obtain reasonable values of the band gap, unphysically large values of U would be needed, much larger than the values of U obtained self-consistently.[46] This may be attributed to the fact that GGA + U itinerant states (those coming mainly from states of the host semiconductor) are still treated at the GGA level and that leads to a total band gap that is underestimated. These itinerant states are more properly treated in GW and, in addition, GGA + U can be seen as an approximation to COHSEX. Therefore, the scheme GGA + U + G_0W_0 has been recently proposed as an alternative to self-consistent GW for systems with d electrons and, particularly, with open d shells.[46]

GGA + U + G_0W_0 clearly improves the GGA + U results. The formation of the IB in Fig. 1(g) is very similar to that from COHSEX + G_0W_0. The value of the splitting between t_{2g} states (0.75 eV) as well as the value of the total band gap (2.5 eV) are, however, smaller that those obtained with GW. For the pure semiconductor, the GGA + G_0W_0 band gap is found to be 2.4 eV; in much better agreement with experiments than that obtained with GW. Although this improvement with respect to GW is because of a cross cancellation of errors (and not because the precision of the method) and because it is sensitive to the value of U, we can conclude that GGA + U + G_0W_0 gives the better quantitative results with an affordable computational cost, and therefore it can be used for the characterization of the compound with a 0.16 normality index.

B. Study of the partially inverse structure

Mg and In atoms have been reordered in order to obtain the desired degree of normality with the following cell: $MgIn_5[Mg_5TiIn_6]S_{24}$, where the square brackets indicate atoms in the octahedral sites and the rest being in tetrahedral sites. The study of the effect of the degree of normality of the $MgIn_2S_4$ host semiconductor has shown that only the band-gap value is affected by the normality, whereas other properties are retained.[20,28] The band gap is found to decrease for smaller degrees of normality.

This can also be seen by comparison of Fig. 1(g) with Fig. 4, which represents the density of states (total and projected) of the cell with 16% normality obtained with the GGA + U + G_0W_0 approach.

In the case of the supercell of Ti in $MgIn_2S_4$ with a 16% normality, we find that the electronic structure of the material does not change significantly with respect to that of normality 0, but an increase in the total band gap is found. This makes both the band gap from the VB to the IB and that from the IB to the CB increase, finding GGA + U + G_0W_0 values of $E_{VI} = 1.61$ eV and $E_{IC} = 1.18$ eV. These values have to be compared with those for the full inverse structure in Table I: 1.18 eV and 0.75 eV. The width of the intermediate band is also modified, changing from 0.61 eV for $x = 0$ to 0.14 eV for $x = 0.16$ as a result of the lower concentration of Ti.

IV. SUMMARY AND CONCLUSIONS

In conclusion, many-body calculations of intermediate-band materials are very cumbersome and are, in general, not feasible for most of them. In particular, the concentrations of transition metals expected to be found experimentally are smaller than those that can be obtained with a 14-atom cell. Nevertheless, self-consistent GW results for the smaller cells have been used to assess the validity of more efficient DFT-based approaches such as GGA + U and GGA + U + G_0W_0.

We find that both the self-consistent parameter-free many-body calculation and GGA + U + G_0W_0 indicate that only a totally occupied intermediate band can be formed by Ti in inverse $MgIn_2S_4$.

This justifies the use of GGA + U + G_0W_0 to treat supercells, as self-consistent GW is not affordable in this case. The occupied IB is the result of a breaking of the degeneracy of the three t_{2g} states resulting from a distortion in the octahedron around the Ti atoms arising from the ordering of Mg and In atoms in the inverse spinel structure of $MgIn_2S_4$. In terms of efficiency of photovoltaic intermediate-band devices, a fully occupied IB requires doping in order to add holes to the IB, since an optimum IB has to be partially filled.

We have found that LDA wave functions and energies are not an accurate starting point for a perturbative G_0W_0 calculation, and that COHSEX or GGA + U are better starting points. In addition, in order to correctly predict the band gaps and splittings of the t_{2g} manifold, GGA + U + G_0W_0 has been shown to be the most accurate approach at a reasonable computational cost. We have thus applied it to the study of a 42-atom supercell with 0.16 degree of normality, finding that the electronic structure of the material does not change significantly with respect to that of normality 0, but an increase in band gaps from the VB to the IB and from the IB to the CB is found.

It will be very valuable to carry out self-consistent GW calculations for other families of IB materials with few atoms in the unit cell to assess whether approaches such as GGA + U + G_0W_0 can be systematically used for the prediction of properties of this type of material.

ACKNOWLEDGMENTS

This work was supported by the Ministerio de Ciencia y Innovacion through the projects Consolider Ingenio 2010 GENESIS-FV (CSD2006-04), FOTOMAT (MAT2009-14625-C03-01) and by the Comunidad de Madrid NUMANCIA 2 project (S-2009ENE-1477). The authors thankfully acknowledge the computer resources, technical expertise, and assistance provided by the Centro de Supercomputación y Visualización de Madrid (CeSViMa) and the Spanish Supercomputing Network.

[1]A. Luque and A. Martí, Phys. Rev. Lett. **78**, 5014 (1997).
[2]P. Olsson, C. Domain, and J.-F. Guillemoles, Phys. Rev. Lett. **102**, 227204 (2009).
[3]P. G. Linares, A. Martí, E. Antolín, and A. Luque, J. Appl. Phys. **109**, 014313 (2011).
[4]E. Antolín, A. Martí, C. Stanley, C. Farmer, E. Cánovas, N. Lopez, P. G. Linares, and A. Luque, Thin Solid Films **516**, 6919 (2008).
[5]K. M. Yu, W. Walukiewicz, W. Shan, J. Wu, J. W. Beeman, M. A. Scarpulla, O. D. Dubon, and P. Becla, J. Appl. Phys. **95**, 6232 (2004); K. M. Yu, W. Walukiewicz, J. W. Ager, D. Bour, R. Farshchi, O. D. Dubon, S. X. Li, I. Sharp, and E. E. Haller, Appl. Phys. Lett. **88**, 092110 (2006); N. Lopez, L. A. Reichertz, K. M. Yu, K. Campman, and W. Walukiewicz, Phys. Rev. Lett. **106**, 028701 (2011).
[6]W. M. Wang, A. S. Lin, and J. D. Phillips, Appl. Phys. Lett. **95**, 011103 (2009).
[7]P. Wahnón and C. Tablero, Phys. Rev. B **65**, 165115 (2002); C. Tablero and P. Wahnón, Appl. Phys. Lett. **82**, 151 (2003).
[8]P. Wahnón, P. Palacios, J. J. Fernández, and C. Tablero, J. Mater. Sci. **40**, 1383 (2005); P. Palacios, J. J. Fernández, K. Sánchez, J. C. Conesa, and P. Wahnón, Phys. Rev. B **73**, 085206 (2006).
[9]K. Sánchez, I. Aguilera, P. Palacios, and P. Wahnón, Phys. Rev. B **79**, 165203 (2009).
[10]G. González-Díaz, J. Olea, I. Mártil, D. Pastor, A. Martí, E. Antolín, and A. Luque, Solar Energy Materials and Solar Cells **93**, 1668 (2009).
[11]B. Bob, A. Kohno, S. Charnvanichborikarn, J. M. Warrender, I. Umezu, M. Tabbal, J. S. Williams, and M. J. Aziz, J. Appl. Phys. **107**, 123506 (2010).
[12]K. Sánchez, I. Aguilera, P. Palacios, and P. Wahnón, Phys. Rev. B **82**, 165201 (2010).
[13]J. Gryko, P. F. McMillan, R. F. Marzke, G. K. Ramachandran, D. Patton, S. K. Deb, and O. F. Sankey, Phys. Rev. B **62**, R7707 (2000).
[14]P. Palacios, K. Sánchez, J. C. Conesa, and P. Wahnón, Phys. Status Solidi A **203**, 1395 (2006).
[15]P. Palacios, I. Aguilera, K. Sánchez, J. C. Conesa, and P. Wahnón, Phys. Rev. Lett. **101**, 046403 (2008).
[16]R. Lucena, I. Aguilera, P. Palacios, P. Wahnón, and J. C. Conesa, Chem. Mater. **20**, 5125 (2008).
[17]P. M. Sirimanne, N. Sonoyama, and T. Sakata, J. Solid State Chem. **154**, 476 (2000).
[18]M. Wakaki, O. Shintani, T. Ogawa, and T. Arai, Jpn. J. Appl. Phys. **19**, 255 (1980).
[19]A. Martí, F. Marrón, and A. Luque, J. Appl. Phys. **103**, 073706 (2008).
[20]I. Aguilera, P. Palacios, K. Sánchez, and P. Wahnón, Phys. Rev. B **81**, 075206 (2010).
[21]L. Hedin, Phys. Rev. **139**, A796 (1965).
[22]F. Bruneval, N. Vast, and L. Reining, Phys. Rev. B **74**, 045102 (2006).
[23]M. Gatti, F. Bruneval, V. Olevano, and L. Reining, Phys. Rev. Lett. **99**, 266402 (2007).
[24]F. Bruneval, N. Vast, L. Reining, M. Izquierdo, F. Sirotti, and N. Barrett, Phys. Rev. Lett. **97**, 267601 (2006).
[25]J. Vidal, S. Botti, P. Olsson, J.-F. Guillemoles, and L. Reining, Phys. Rev. Lett. **104**, 056401 (2010).
[26]J. Vidal, F. Trani, F. Bruneval, M. A. L. Marques, and S. Botti, Phys. Rev. Lett. **104**, 136401 (2010).
[27]S. V. Faleev, M. van Schilfgaarde, and T. Kotani, Phys. Rev. Lett. **93**, 126406 (2004).
[28]M. Marinelli, S. Baroni, and F. Meloni, Phys. Rev. B **38**, 8258 (1988).
[29]M. Wakaki, O. Shintani, T. Ogawa, and T. Arai, Jpn. J. Appl. Phys. **21**, 958 (1982).
[30]L. Gastaldi and A. Lapiccirella, J. Solid State Chem. **30**, 223 (1979).
[31]X. Gonze, J.-M. Beuken, R. Caracas, F. Detraux, M. Fuchs, G.-M. Rignanese, L. Sindic, M. Verstraete, G. Zerah, F. Jollet, M. Torrent, A. Roy, M. Mikami, P. Ghosez, J.-Y. Raty, and D.C. Allan, Comput. Mater. Sci. **25**, 478 (2002); X. Gonze, G.-M. Rignanese, M. Verstraete, J.-M. Beuken, Y. Pouillon, R. Caracas, F. Jollet, M. Torrent, G. Zerah, M. Mikami, Ph. Ghosez, M. Veithen, J.-Y. Raty, V. Olevano, F. Bruneval, L. Reining, R. W. Godby, G. Onida, D. R. Hamann, and D. C. Allan, Z. Kristallogr. **220**, 558 (2005).
[32]G. B. Bachelet, D. R. Hamann, and M. Schluter, Phys. Rev. B **26**, 4199 (1982).
[33]M. Fuchs and M. Scheffler, Comput. Phys. Commun. **119**, 67 (1999).
[34]M. S. Hybertsen and S. G. Louie, Phys. Rev. B **34**, 5390 (1986).
[35]R. W. Godby and R. J. Needs, Phys. Rev. Lett. **62**, 1169 (1989).
[36]G. Kresse and J. Hafner, Phys. Rev. B **47**, RC558 (1993); G. Kresse and J. Furthmüller, *ibid.* **54**, 11169 (1996); VASP code, [http://cms.mpi.univie.ac.at/vasp].
[37]J. P. Perdew, J. A. Chevary, S. H. Vosko, K. A. Jackson, M. R. Pederson, D. J. Singh, and C. Fiolhais, Phys. Rev. B **46**, 6671 (1992); J. P. Perdew and Y. Wang, *ibid.* **45**, 13244 (1992).
[38]G. Kresse and D. Joubert, Phys. Rev. B **59**, 1758 (1999); P. E. Blöchl, *ibid.* **50**, 17953 (1994).
[39]See Supplemental Material at http://link.aps.org/supplemental/10.1103/PhysRevB.84.115106 for the comparisons leading to this conclusion.
[40]M. Cococcioni and S. de Gironcoli, Phys. Rev. B **71**, 035105 (2005).
[41]K. Sánchez, P. Palacios, and P. Wahnón, Phys. Rev. B **78**, 235121 (2008).
[42]Kefrén Sánchez, Ph.D. thesis, p. 137, Universidad Politéctica de Madrid, 2009.
[43]M. van Schilfgaarde, T. Kotani, and S. Faleev, Phys. Rev. Lett. **96**, 226402 (2006).
[44]J. Ruiz-Fuertes, D. Errandonea, F. J. Manjón, D. Martínez-García, A. Segura, V. V. Ursaki, and I. M. Tiginyanu, J. Appl. Phys. **103**, 063710 (2008).
[45]M. J. Lucero, I. Aguilera, C. V. Diaconu, P. Palacios, P. Wahnón, and G. E. Scuseria, Phys. Rev. B **83**, 205128 (2011).
[46]H. Jiang, R. I. Gomez-Abal, P. Rinke, and M. Scheffler, Phys. Rev. B **82**, 045108 (2010).